Neuron, Vol. 18, 29–42, January, 1997, Copyright ©1996 by Cell Press

Mice Lacking p35, a Neuronal Specific Activator of Cdk5, Display Cortical Lamination Defects, Seizures, and Adult Lethality

Teresa Chae,*‖ Young T. Kwon,*‖ Roderick Bronson,† Pieter Dikkes,‡ En Li,§ and Li-Huei Tsai*
*Department of Pathology
Harvard Medical School
Boston, Massachusetts 02115
†U.S. Department of Agriculture
Human Nutrition Research Center on Aging
and Department of Pathology
Tufts University Schools of Veterinary Medicine
Boston, Massachusetts 02111
‡Department of Neurology
Division of Neuroscience
Children's Hospital
Boston, Massachusetts 02115
§Cardiovascular Research Center
Massachusetts General Hospital
Department of Medicine
Harvard Medical School
Charlestown, Massachusetts 02129

Summary

The adult mammalian cortex is characterized by a distinct laminar structure generated through a well-defined pattern of neuronal migration. Successively generated neurons are layered in an "inside-out" manner to produce six cortical laminae. We demonstrate here that p35, the neuronal-specific activator of cyclin-dependent kinase 5, plays a key role in proper neuronal migration. Mice lacking p35, and thus p35/cdk5 kinase activity, display severe cortical lamination defects and suffer from sporadic adult lethality and seizures. Histological examination reveals that the mutant mice lack the characteristic laminated structure of the cortex. Neuronal birth-dating experiments indicate a reversed packing order of cortical neurons such that earlier born neurons reside in superficial layers and later generated neurons occupy deep layers. The phenotype of p35 mutant mice thus demonstrates that the formation of cortical laminar structure depends on the action of the p35/cdk5 kinase.

Introduction

Mammalian corticogenesis follows highly regulated spatial and temporal patterns of neuronal differentiation and migration to generate the characteristic cortical laminae. During corticogenesis, neurons that will occupy the cortex arise from progenitor cells that line the lateral ventricle in the ventricular and subventricular zones. Postmitotic neurons leave the ventricular zone and migrate along radial glial fibers through the intermediate zone before taking up residence in the cortical plate. Migrating neurons move past earlier generated neurons to take more superficial positions in the cortical plate. The continuation of this migration process throughout cortical development leads to the so-called "inside-out" generation of cortical layers (Angevine and Sidman, 1961; Luskin and Shatz, 1985). Although the migratory patterns of neurons generated throughout corticogenesis have been studied in great detail, the molecular basis for migration of cortical neurons is poorly understood.

Cyclin-dependent kinase 5 (cdk5) is highly related to the family of cyclin-dependent kinases known to function throughout the cell division cycle (Hellmich et al., 1992; Lew et al., 1992; Meyerson et al., 1992). Despite its homology to the cdk's, a role for cdk5 in cell cycle division has yet to be elucidated. In adult mice, high levels of cdk5 protein and kinase activity are detected in brain extracts (Tsai et al., 1993). Cdk5 kinase activity has been shown to phosphorylate neurofilaments and microtubule-associated protein tau (see review by Lew and Wang, 1995). Examination of cdk5 during embryogenesis revealed that cdk5 protein and kinase activity increase as forebrain development progresses, while cdc2 and its kinase activity decrease over the same period. Cdk5 kinase activity depends on binding of p35, a highly specific regulatory subunit, identified by virtue of its in vivo association with cdk5 in neurons (Lew et al., 1994; Tsai et al., 1994). p35 is a novel protein with no significant homology to previously identified proteins or the known class of cdk regulatory subunits, the cyclins. It exhibits complete specificity in binding and activating cdk5 despite the high degree of homology between cdk5 and the other cdk's.

p35 is highly expressed in postmitotic neurons but is completely absent in proliferating neuronal progenitors (Tsai et al., 1994; Delalle et al., 1997). Throughout embryonic neuronal development, p35 mRNA is present at robust levels in the cell soma as well as the axonal tracts of the entire central nervous system (CNS). In the developing mouse cortex, p35 mRNA is present in postmitotic migrating neurons as well as those occupying the cortical plate. Furthermore, immunohistochemical studies on developing rat cortex indicate that p35 is present in neuronal cell bodies and fiber pathways such as the corpus callosum and external capsule (Tomizawa et al., 1996). In adult rodents, p35 expression is diminished in most compartments of the CNS except for the forebrain where the level of p35 is maintained. In cultured cortical neurons from rat embryos, p35 and cdk5 were shown to be localized to the cell body and processes and enriched in the tips of growing axons (Nikolic et al., 1996). Moreover, neurite outgrowth in these cultured cortical neurons was inhibited upon introduction of a dominant negative mutant of cdk5 by transfection, indicating a role of cdk5 in neurite growth (Nikolic et al., 1996). Together, the expression and in vitro functional studies of p35 and cdk5 suggest that the p35/cdk5 kinase plays a role in dynamic, developmental neuronal processes.

To test the hypothesis that the p35/cdk5 kinase may play an essential role in neuronal development and to examine the developmental consequences of losing p35 function, we have generated mice lacking p35. Our studies on p35 knockout mice elucidate a critical role of

‖These authors contributed equally to this work.

p35 in the proper organization of cortical structures. Histological examination revealed major defects in the developing neocortex where the normal lamination pattern of the cortical neurons is disrupted. In addition, certain axonal trajectories and dendritic structures are altered in p35 mutant mice. Furthermore, we demonstrate that the abnormal patterning of the cortex is due to a defect in neuronal migration. Finally, we show that p35 mutant mice are prone to develop fatal seizures. The phenotype of p35 mutant mice provides the first evidence for an intracellular kinase activity regulating the migration and hence the laminar fate of neurons during cortical development.

Results

Generation of p35 Mutant Mice

Cloning of the *p35* genomic locus from a 129/Sv mouse liver genomic DNA library revealed that *p35* has a continuous coding region without interruption by intron sequences. To delete the genomic *p35* locus by homologous recombination (Capecchi, 1989; Mansour et al., 1988), we created a *p35* targeting construct by replacing the entire *p35* coding region with the neomycin resistance (neo^R) gene in the opposite transcriptional orientation (Figure 1A). Embryonic stem (ES) cells were transfected with the targeting construct and selected in media containing both G418 and FIAU for homologous recombination events at the *p35* locus. Southern blot analysis revealed that among the 176 ES clones selected, 6 had undergone homologous recombination (data not shown). Two *p35* heterozygous clones (6D3 and 4C4) were used to generate chimeric animals. Male chimeras displaying nearly 100% agouti coat color were mated to C57BL/6 females to produce F1 offspring carrying germ-line transmission of the mutated *p35* allele. Male and female F1 *p35* heterozygotes (+/−) were intercrossed to generate F2 homozygous (−/−) mutants, as demonstrated by Southern blotting (Figure 1B). Chimeras of one clone were bred to 129/Sv females to generate mutant mice of the 129/Sv inbred background (see Experimental Procedures). Although mice derived from clone 6D3 of a mixed genetic background (129/Sv/C57BL/6) were analyzed in depth, the phenotypes described here were also observed in mice derived from clone 4C4 and clone 6D3 in the 129/Sv inbred background.

Heterozygous intercrossing resulted in wild-type, heterozygous, and homozygous mutant progeny in the expected ratios of 1:2:1. Whole-brain lysates of each genotype were analyzed for the presence of p35 by Western blot analysis and histone H1 kinase assays. Using an affinity-purified rabbit polyclonal antibody to p35 for Western blotting, p35 is not detectable in brain lysates derived from homozygous mutants, and its abundance in heterozygous mutants is half that of wild type (Figure 1C). Adult brain lysates were also immunoprecipitated with a p35 or cdk5-specific antibody followed by an in vitro kinase assay in the presence of histone H1. Similar to the results of Western blot analysis, p35-associated histone H1 kinase activity is not detectable in the brain lysates of homozygous mutants and is present at approximately half of the wild-type level in the heterozygous brain lysates (Figure 1D). Cdk5-associated histone H1 kinase activity is also undetectable in $p35^{-/-}$ brain lysates (Figure 1E). These results confirm that the *p35* locus is completely deleted and that no p35 protein product is made in the homozygous mutant animals. Furthermore, p35 appears to be the major regulatory subunit of cdk5 in adult brain lysates as cdk5-associated histone H1 kinase activity is undetectable in $p35^{-/-}$ lysates. Despite the lack of p35, the viability of mice during embryonic and neonatal development is not affected.

Disrupted Cortical Patterning in p35 Mutant Mice

$p35^{-/-}$ males and females do not show gross anatomical abnormalities or defects in somatic organs or tissues (data not shown). Mutant mice feed normally and are indistinguishable from wild-type or heterozygous mutant littermates with regard to body weight, rearing, and grooming. Although the appearance of homozygous mutant mice is largely normal, they are in general more outwardly docile and calm. Histological analysis revealed severe defects in the patterning of the cerebral cortex and to a lesser extent in the hippocampus, olfactory bulb, and cerebellum of p35 mutant mice.

The size, shape, and surface of the brain are indistinguishable between the wild-type and p35 mutant mice (data not shown). However, coronal sections of brains prepared from 3-month-old animals reveal a general disorganization of the forebrain. At low magnification, it is apparent that the structure of the p35 mutant forebrain differs from that of wild type (Figures 2A and 2B). For instance, the lateral ventricles in the p35 mutant forebrain are about twice the size of the ventricles in the wild-type forebrain, and these dilated ventricles seem to be created at the expense of the septum, which is reduced in size, especially at the junction between the septum and the corpus callosum. The size of the striatum is also reduced in the mutant forebrain. In addition, the p35 mutant cortex exhibits a much reduced corpus callosum.

Further examination of the neocortical structure under higher magnification reveals two striking differences between wild-type and p35 mutant mice. In the cortex of wild-type mice, six laminae are apparent and can be distinguished by packing density as well as neuronal morphology (Figure 2C). This laminated structure of the neocortex is not apparent in p35 mutant mice (Figure 2D). Layer I, which contains Cajal-Retzius cells but is relatively cell-free, is still present. However, layers II and III, which ordinarily consist predominantly of small pyramidal cells, are instead occupied by large pyramidal neurons normally present in layer V. Based on their morphological features, we have identified pyramidal, granule, and polymorphic cells of layers II/III, IV, and VI respectively, in the p35 mutant cortex but find no recognizable pattern in their distribution (Figure 2D). Despite the abnormality of neuronal patterning, overall cell density is comparable between wild-type and p35 mutant mice (22 cells/100 μm^2 for $p35^{+/+}$; 21.5 cells/100 μm^2 for $p35^{-/-}$). The defects in lamination are less severe in the more lateral-ventral region of the cortex, and the organization of the entorhinal and pyriform cortex appears to be largely intact (data not shown).

To examine the cortical defects more closely, cortices

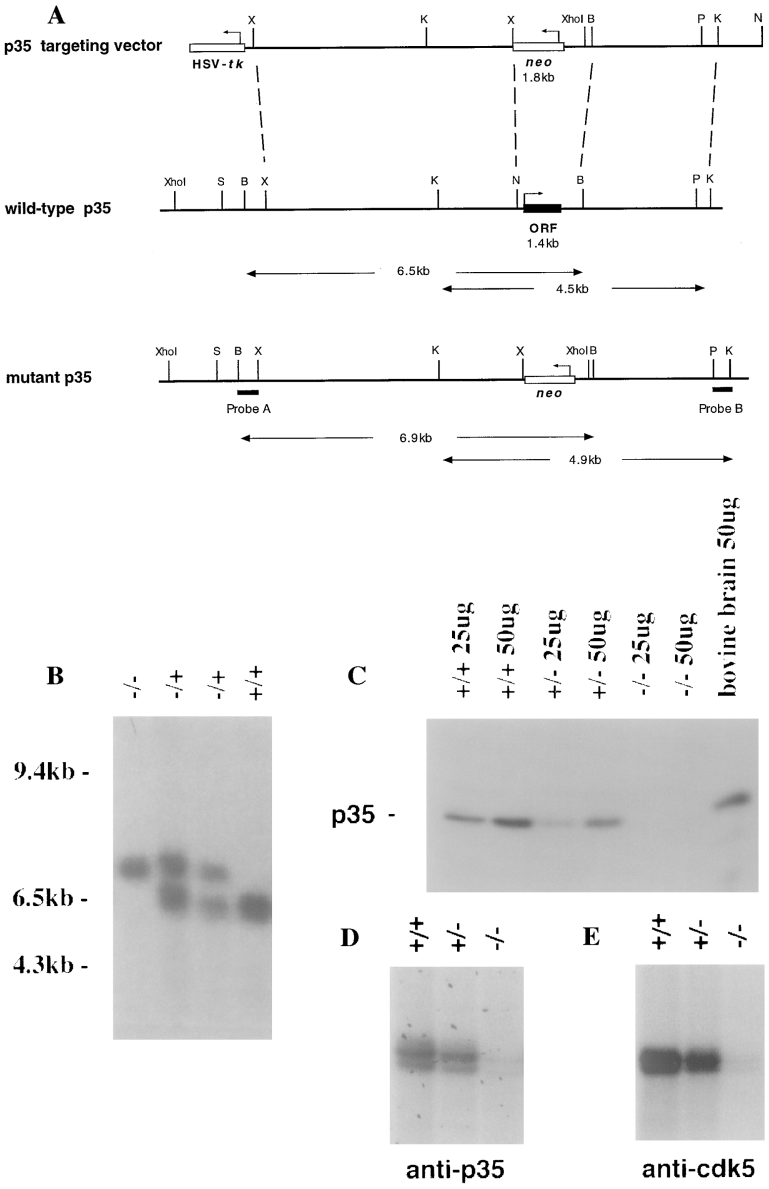

Figure 1. Production of p35 Mutant Mice

(A) Targeted deletion of the *p35* open reading frame: 1.4 kb of the *p35* locus including the entire open reading frame (ORF) was replaced in the targeting vector with the 1.8 kb neomycin resistance gene (neo) in the opposite orientation. A total of 8 kb of sequence homology exists between the targeting vector and wild-type locus as delineated by dashed lines. The 400 bp increase in size due to the insertion of the neo cassette allowed the mutant and wild-type loci to be distinguished by Southern blot. The position of probes A and B used for Southern blot analysis are indicated. Probe A, a 400 bp BamHI-XbaI fragment external to the region of homology contained within the targeting construct, detects 6.5 kb and 6.9 kb BamHI fragments from the wild-type and mutant alleles, respectively. Probe B, a PstI-KpnI 500 bp fragment contained within the homologous regions, detects 4.5 kb and 4.9 kb KpnI fragments from the wild-type and mutant alleles, respectively. Restriction sites are as follows: B, BamHI; K, KpnI; N, NotI; P, PstI; S, SalI; and X, XbaI.

(B) Genotyping of four 3-week-old littermates. Southern blot of tail DNA with probe A reveals a 6.5 kb BamHI fragment from the wild-type allele and a 6.9 kb BamHI fragment from the mutant allele.

(C) Absence of p35 protein in $p35^{-/-}$ mice. Western blot of wild-type, +/−, and −/− whole-brain lysates using an affinity-purified rabbit polyclonal antibody for p35. Bovine brain lysate is shown as a positive control.

(D) Absence of p35-associated kinase activity in $p35^{-/-}$ mice. Whole-brain lysate (1 mg) of +/+, +/−, and −/− 4-week-old mice were immunoprecipitated with a monoclonal antibody specific for p35 and assayed for histone H1 kinase activity.

(E) Absence of cdk5-associated kinase activity in $p35^{-/-}$ mice: 500 μg of brain lysates used for (D) were immunoprecipitated with a polyclonal antibody against cdk5 and assayed for histone H1 kinase activity.

of 3-month-old animals were analyzed by Golgi impregnation, which selectively labels a subset of neurons and their dendritic arbors. In the wild-type cortex, radially arrayed apical dendrites elaborated from pyramidal neurons are evident (Figures 3A and 3C). The p35 mutant cortex, however, differs from the wild type in several respects. First, the radial distribution of the pyramidal neurons and their apical dendrites is not conspicuous (Figure 3B), and no recognizable pattern of neuronal arrangement is apparent in the p35 mutant cortex. In addition, the orientation of the neuronal soma and the direction of dendritic growth are altered (Figure 3D). Again, these differences in the orientation of p35 mutant pyramidal neurons appear to be more severe in the medial neocortex than the lateral-ventral cortical region, as apical dendrites are evident in the entorhinal and pyriform cortex (data not shown).

Nissl and myelin staining indicate that in addition to the apparent lamination abnormality, the p35 mutant cortex contains aberrant fiber fascicles as well (Figure 2D). Using a modified silver staining technique to impregnate fibers (Fink and Heimer, 1967; Schneider, 1969), it is possible to identify fiber fascicles coursing throughout the cortex of the p35 mutant, giving it a mesh-like appearance (Figure 3F), while these fiber fascicles are totally absent in the wild-type cortex (Figure 3E). These aberrant fiber fascicles are only conspicuous in the neocortex and are not apparent in the lateral-ventral portion of the cortex of the p35 mutant. While the thickness of the corpus callosum is much reduced in the p35 mutant (Figures 3E and 3F), the internal capsule, rostral commissure, optic chiasm, corticohabenular tract, and fornix do not appear to be grossly affected.

In addition to the disruption of the cortical structure, there are mild distortions in the organization of the hippocampus, the olfactory bulb, and the cerebellum of

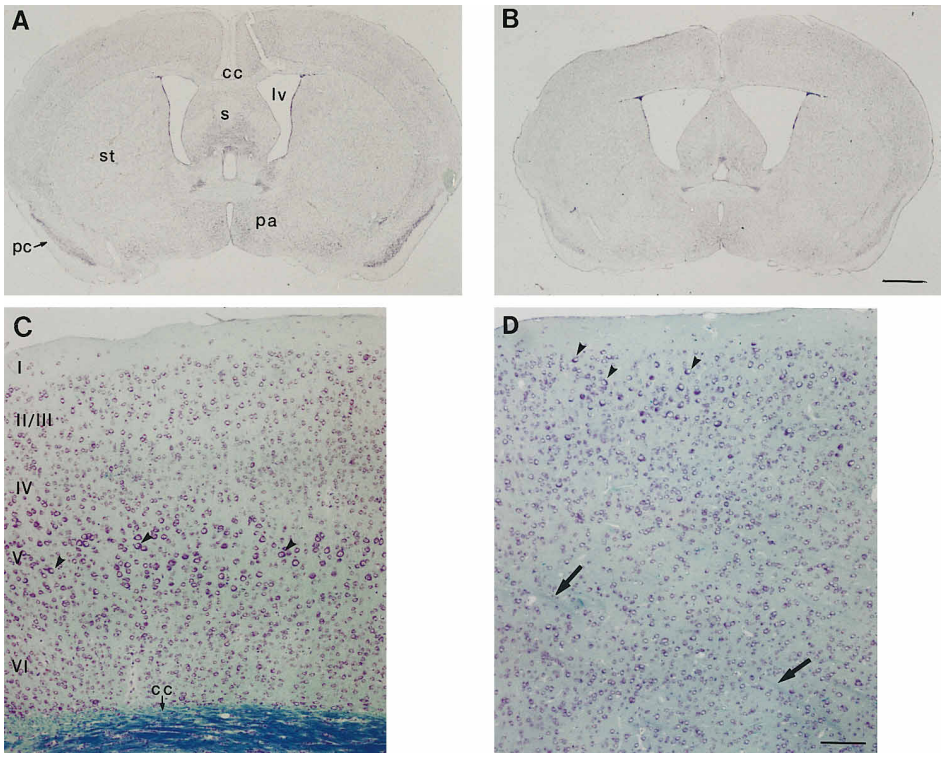

Figure 2. Gross Structural Abnormalities and Disrupted Cortical Structure in p35 Mutant Mice

Coronal sections at the level of anterior commissure of the p35 mutant cortex (B and D) are compared with those of wild-type cortex (A and C) after cresyl violet (A and B) or cresyl violet and luxol fast blue staining (C and D). At low magnification (10×, A and B), the p35 mutant cortex displays dilated lateral ventricles (lv) and reduced size of the septum (s), striatum (st), and corpus callosum (cc). The configuration of the pyriform cortex (pc) and the preoptic areas (pa) appears to be intact in the mutant cortex. At high magnification (90×, C and D), the six regular laminae present in the wild-type cortex (C) are not apparent in the p35 mutant cortex (D). The large pyramidal neurons characteristic of layer V are present in the superficial layers of the mutant cortex (arrowheads). The mutant cortex contains aberrant fiber fascicles that are not present in the wild-type cortex (arrows). Scale bar = 1 mm (A and B) or 100 μm (C and D).

the p35 mutant mice. In the hippocampus and dentate gyrus, the majority of cells are included in a laminar structure reminiscent of wild type, though they are less densely packed and are interrupted at points (Figures 4A and 4B). Some hippocampal neurons and granule cells of the dentate gyrus are also scattered in the plexiform layers. In the olfactory bulb of the p35 mutant, the internal plexiform layer between the mitral cell and internal granule layers is absent (Figures 4C and 4D). Instead, the area that would normally consist of the internal plexiform layer is populated with cells morphologically resembling granule cells. In addition, the internal granule layer lacks the laminar configuration apparent in the wild type. The p35 mutant cerebellum displays a normal gross morphology, and the folia and laminated structure are similar to those of wild-type mice. However, the molecular layer in p35 mutant mice exhibits greater cell density than wild type and is occupied by cells resembling granule cells (Figures 4E and 4F). In some regions, Purkinje cells are located ectopically within the granule cell layer (data not shown). The patterning and appearance of other CNS structures including the thalamus, midbrain, medulla, and spinal cord as well as the peripheral nervous system are unaffected by the lack of p35 (data not shown).

Histological analysis has also been conducted on the p35 homozygous mutants generated from the second ES clone (4C4) as well as mutants of the inbred 129/Sv background. All abnormal features described in mice of the mixed background are also evident in animals of the inbred background. In addition, mutant mice produced from the second ES clone display identical defects. These observations further confirm that the histological abnormalities of p35 mutant animals are the consequence of the absence of functional p35 gene product.

Analysis of Embryonic Brains

Histological examination of the adult p35 mutant cortex revealed defects in cytoarchitectonic formation, particularly in cortical lamination and in the trajectory of certain axonal tracts. To determine the onset of these defects and to define the mechanism underlying the observed abnormalities, we studied histogenesis of the embryonic brains. Mouse corticocytogenesis takes place between embryonic day 11 (E11) and E17. Proliferation of the neural progenitors is confined primarily to the ventricular zone, and postmitotic neurons migrate to the cortical plate through the intermediate zone. To assess the proliferation profile of p35 mutant neuronal progenitors, embryos were pulse labeled in utero with bromodeoxyuridine (BrdU), which is incorporated into the DNA of dividing cells. At E13, the thickness (100 μm from pial

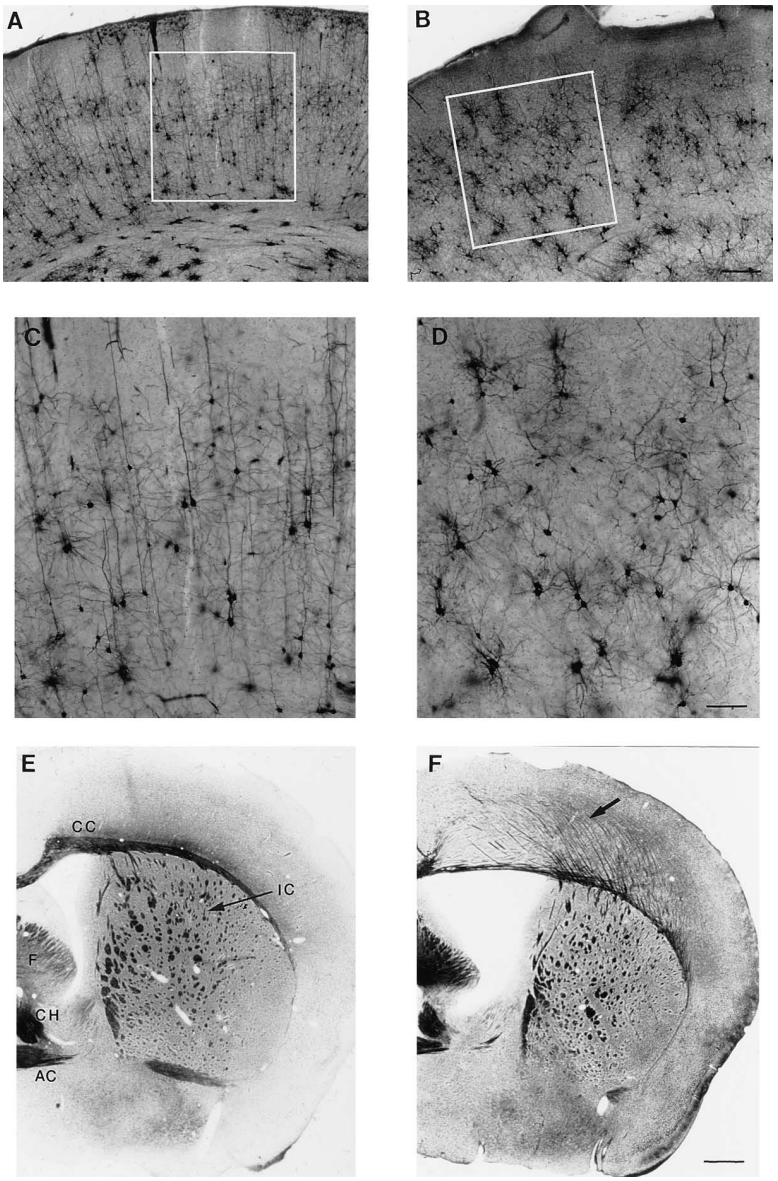

Figure 3. Altered Cell Orientation, Dendritic, and Axonal Trajectories in p35 Mutant Mice

Golgi impregnation of wild-type (A and C) and p35 mutant (B and D) coronal sections at the level of anterior hippocampus of the cortex reveals that radially aligned apical dendrites are not apparent in the p35 mutant cortex. At higher magnification of the white boxed area in (A) and (B), the altered orientation of pyramidal neurons in the p35 mutant cortex is evident (C and D). Silver staining of coronally sectioned wild-type (E) and mutant (F) cortices at the level of anterior commisure illustrates the aberrant mesh-like fiber fascicles (thick arrow) and reduced corpus callosum (CC) in the p35 mutant cortex. The internal capsule (IC), anterior commissure (AC), and corticohabenular tract (CH) appear relatively normal in the p35 mutant cortex. Scale bar = 125 μm (A and B), 60 μm (C and D), or 500 μm (E and F). Midline lies to the right (A, B, C and D) and to the left (E and F).

to ventricular surface for both genotypes in the medial region of the cerebral wall) and cell density of the cerebral wall as well as the number of BrdU-positive cells in the ventricular zone (53.5 cells/100 μm^2 for $p35^{+/+}$; 55.3 cells/100 μm^2 for $p35^{-/-}$) are similar between wild type and mutant (Figures 5A and 5B). At E15, however, differences in the structure of the developing cortex are apparent (Figures 5C and 5D). Although the thickness of the developing cerebral wall from dorsal to ventral is comparable between wild type and mutant, the $p35^{-/-}$ cortical plate is thinner (30%–50% less than wild type) and the intermediate zone contains more cells (73.3 cells/100 μm^2 for $p35^{+/+}$; 111.1 cells/100 μm^2 for $p35^{-/-}$). The increased density of cells in the p35 mutant intermediate zone is not likely due to increased proliferation of progenitor cells, as the number of BrdU-positive cells in the ventricular zone is similar between wild type and mutant at E15 (22.1/100 μm^2 for $p35^{+/+}$; 22.6/100 μm^2 for $p35^{-/-}$). These differences in structure between wild-type and p35 mutant cortex are also apparent at E17 and E18.5 (data not shown).

One possible mechanism to explain the abnormal cytoarchitectural pattern of the E15 $p35^{-/-}$ cerebral wall is that the radial glial fibers, which guide postmitotic neurons during their migration, are altered or absent in p35 mutant mice. To examine the radial glial fiber system, E17 cortices were stained with the monoclonal antibody RC2 (Misson et al, 1988). At E17, the RC2 antibody stains radial glial fibers in the cerebral wall, which run a course perpendicular to the pial surface. As seen in Figures 5E and 5F, the alignment and density of radial glial fibers are comparable between wild-type and mutant E17 cortices. The integrity of radial glial fibers in p35 mutant mice is consistent with observations that p35 is not expressed in glial cells (Tsai et al., 1994; Tomizawa et al., 1996). These data suggest that the

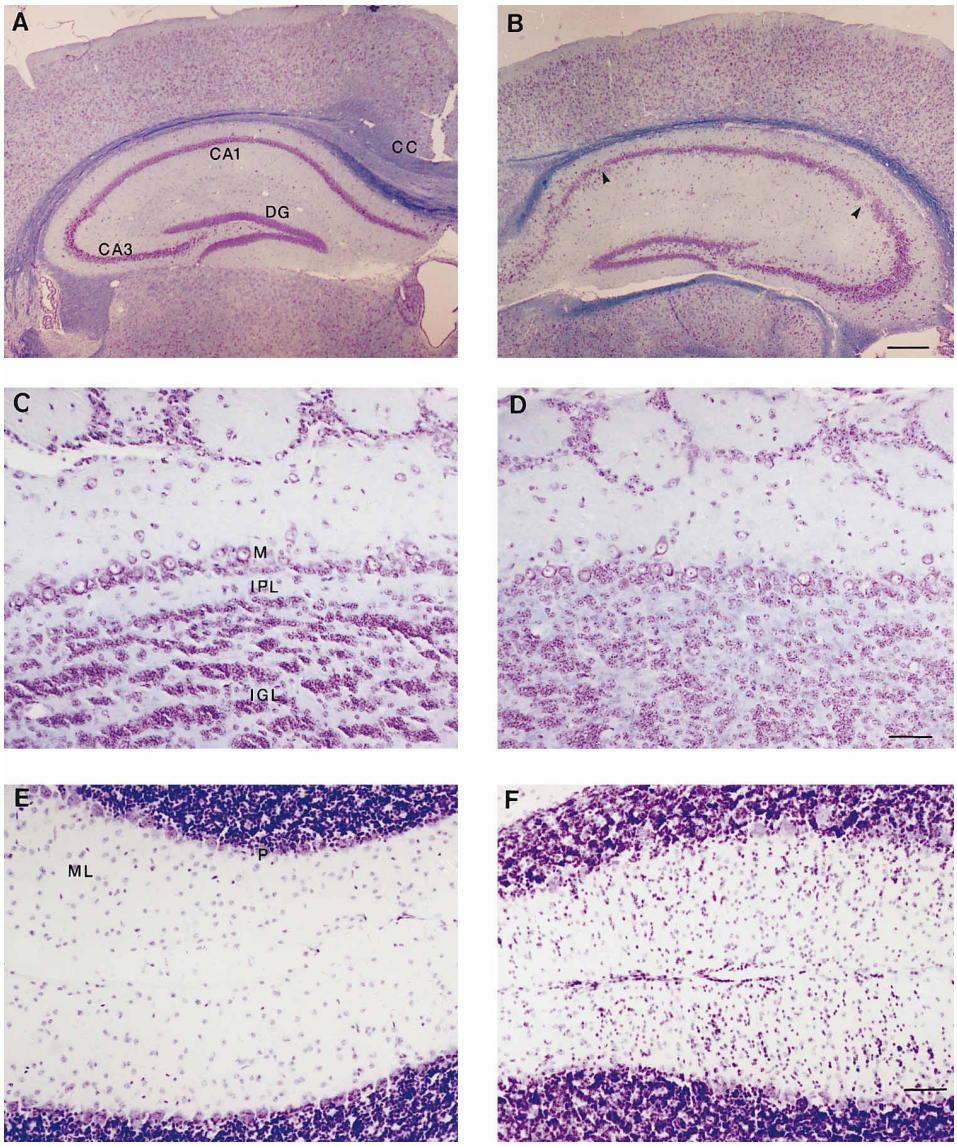

Figure 4. Mild Distortion of Several CNS Structures in p35 Mutant Mice

Cresyl violet and luxol fast blue stained coronal sections of the hippocampal formation (A and B), olfactory bulb (C and D), and cerebellum (E and F) are compared between wild-type (A, C, and E) and p35 mutant (B, D, and F) mice. In the hippocampal formation, neurons in CA1, CA3, and dentate gyrus (DG) are less densely packed and are interrupted at points (arrow heads) in the p35 mutant mouse. In the mutant olfactory bulb, no clear internal plexiform layer (IPL) is present between the mitral cells (M) and internal granule layer (IGL). In the cerebellum, cell density of the molecular layer (ML) is higher in the mutant than the wild type. Scale bar = 250 μm (A and B), 50 μm (C and D), or 100 μm (E and F). Midline lies to the left (A) and to the right (B).

abnormal cortical lamination of p35 mutant animals is not likely to be the consequence of a disrupted radial glial fiber system.

Neuronal Birth-Dating Analyses

Although the higher cell density in the intermediate zone of the p35 mutant embryonic cerebral wall (Figure 5D) indicates a possible defect in cell migration, we cannot rule out the possibility of a cell fate defect during corticogenesis. It has been well documented that the laminar structure of the cortex is built by the migration of successively generated neurons in an inside-to-outside fashion, such that earlier born neurons reside in deeper layers while neurons born later occupy more superficial layers. As shown in Figures 2C and 2D, the large pyramidal neurons that normally localize to layer V are present in layers II/III of the p35 mutant cortex. Thus, either the p35 mutant neurons migrate abnormally or the birth dates of the various classes of neurons are altered such that the large pyramidal neurons of layer V are born toward the end of corticocytogenesis. To distinguish between the two possibilities, we labeled E13 and E16 embryos with BrdU and examined the localization of BrdU-positive cortical neurons in 1-month-old animals. As illustrated schematically in Figure 6A, if the abnormal lamination is due to birth-dating defects, BrdU-labeled neurons should appear in comparable laminae in the

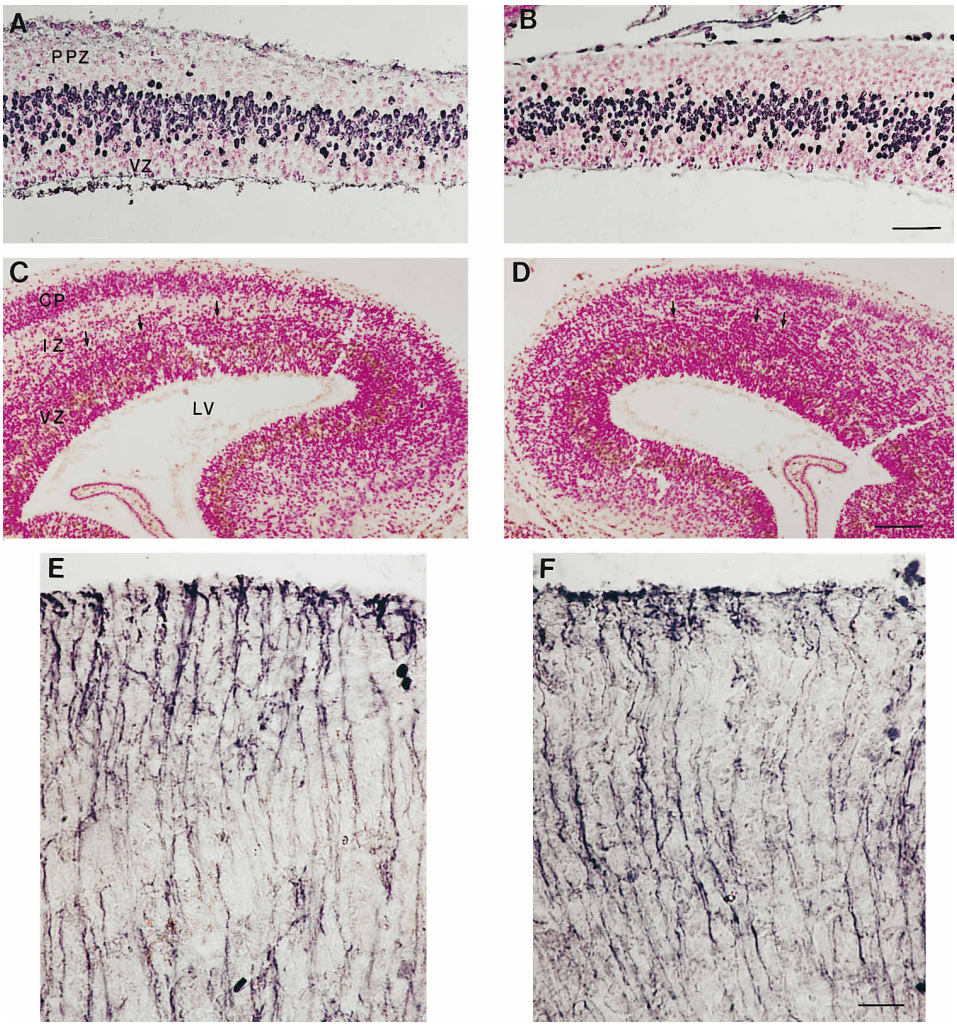

Figure 5. Configuration of the p35 Mutant Brain During Embryonic Development

Coronal sections of BrdU pulse-labeled E13 (A and B) and E15 (C and D) cerebral walls are compared. Sections were counterstained with basic fuchsin (A–D). The number of BrdU positive cells are comparable between wild-type (B and C) and mutant (A and D) cortices in both E13 and E15 embryos (see text). The structure and cell density of postmitotic cell layers above the ventricular zone (VZ) are similar between wild-type and mutant at E13. However, at E15, the mutant cortex displays higher cell density in the intermediate zone (IZ) and a thinner cortical plate (CP). BrdU-labeled postmitotic neurons migrating out of the ventricular zone can be seen in wild-type (C) and p35 mutant (D) cortices (arrows). RC2 staining of E17 cortices (E and F) reveals that the pattern and distribution of radial glial fibers is comparable between wild-type and p35 mutant mice in the cortex. Scale bar = 50 μm (A, B, E, and F); 100 μm (C and D).

wild-type and p35 mutant cortices. Conversely, if neuronal migration is affected, neurons labeled at the same time should end up in different laminae in wild-type and mutant mice. When E13 progenitors are labeled, BrdU-positive cells are present in a broad area in the lower half of the neocortex corresponding to layers IV, V, and VI in the wild-type cortex (Figure 6B), an observation consistent with previous reports (Caviness, 1982; Caviness and Sidman, 1973). In the p35 mutant cortex, however, the majority of BrdU-labeled cells are found primarily in superficial layers of the cortex, though labeled cells are also apparent in the deeper layers of the cortex (Figure 6C). A quantitative comparison of the distribution of E13 BrdU-labeled neurons between wild type and p35 mutant is depicted in Figure 6F. When E16 progenitors are labeled, BrdU-positive cells are confined to layers II/III of the wild-type cortices (Figure 6D). In the p35 mutant cortex, however, BrdU-labeled cells are apparent primarily in deep layers of the cortex, with some labeled cells occupying more superficial layers (Figure 6E). Figure 6G depicts the quantitative difference in distribution of E16 BrdU-labeled neurons between wild-type and mutant cortices. Together, the E13 and E16 birth-dating experiments largely rule out the possibility of a cell fate defect while they reveal an inverted packing pattern of neurons during cortical development in the p35 mutant mouse.

Seizure and Lethality of p35 Mutant Mice

Throughout the course of our analysis of *p35*$^{-/-}$ mice, approximately 15% of homozygous mutants have died unexpectedly while none of the wild-type or heterozygous littermates have died. Male and female *p35*$^{-/-}$ mice die with an equal frequency, and death occurs from 3

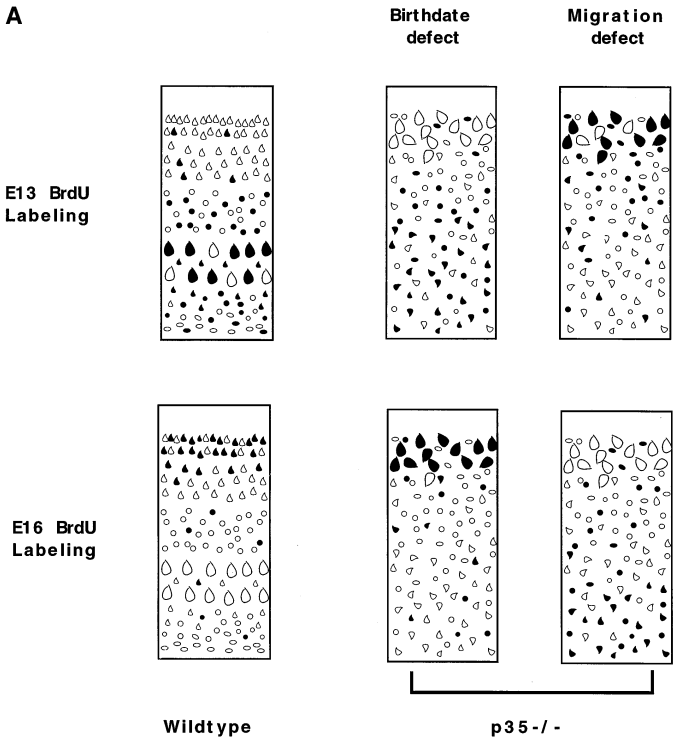

(*Figure 6 continued on next page*)

Figure 6. Inverse Packing Pattern of p35 Mutant Neurons During Cortical Development

(A) Schematic illustration of neuronal birthdating experiments demonstrating the contrasting results of a potential birth date or cell fate defect versus a migration defect. Filled cells represent BrdU-labeled cells. BrdU was injected into E13 or E16 timed pregnant females. Coronal sections of the cortex at the level of anterior hippocampus were obtained from 1-month-old wild-type and p35 mutant offspring and stained for BrdU. The E13 birthdating experiment shows that in the wild type (B), heavily labeled neurons are present in the lower half of the cortex while in the p35 mutant (C), a majority of the labeled neurons are present in the superficial layers although some labeled neurons can also be found in the deeper layers. The E16 birth-dating experiment shows that in wild-type (D), labeled neurons are present in the superficial layers while in the p35 mutant (E), most of the labeled neurons are present in the deeper layers of the cortex although some labeled neurons are also present in the more superficial layers. These sections were counterstained with cresyl violet. Histograms of the E13 birthdating experiment (F) and the E16 experiment (G) illustrate the percentage of total BrdU-labeled cells in each cortical layer in the wild type and the area corresponding to these layers in p35 mutant sections. Each column represents the average of at least three independent sections counted. Standard deviation is presented in Experimental Procedures. Corpus callosum (CC); 90× (B–E).

weeks of age onward. Autopsy of five animals revealed no evidence of tumors or obvious illness in somatic tissues, and examination of the brains of these animals revealed no evidence of hemorrhaging or other damage.

Considering the improperly formed laminar structure of the cortex and the pattern of aberrant fibers within it, one reasonable proposal to explain the unexpected death is that the altered cortical structure causes the p35 mutant mice to have an increased susceptibility to seizures. During long-term observation of these animals, we found that the p35 mutant mice suffer from seizures. These observations of naturally occurring seizures prompted us to ask whether p35 mutant mice have a greater tendency for fatal seizures. To test experimentally if p35 mutant mice have a lower threshold for seizure-induced lethality, seizures were induced in wild-type and mutant animals using the chemical convulsant pentylenetetrazol (PTZ). PTZ induces generalized convulsions in rodents with a characteristic dose responsiveness (Ben-Ari et al., 1981) and has been used extensively in studies of seizure-induced *c-fos* expression in the CNS (Morgan et al., 1987; Morgan and Curran, 1991). Both genders of wild-type and p35 mutant mice aged 9 to 14 weeks were tested. Administration of PTZ at 30 mg/kg body weight, a dose which generally does not induce observable seizure activity in mice, led to no observable seizure activity in wild-type or mutant animals (data not shown). Administration of PTZ at 50 mg/kg body weight, a nonlethal dose to wild-type mice, led to a single generalized convulsion in mice of both genotypes, characterized by a rapid progression of behavior starting with loss of posture, then myoclonic jerks, followed by hyperextension of the neck and trunk, which was associated with cycling motions of the limbs

Table 1. Summary of PTZ-Induced Seizure Experiments

Genotype	Total Mice	Number of Generalized Convulsions	Number of Deaths	% Experiencing Generalized Convulsions	% Death
Trial 1					
+/+	6	3	0	50	0
−/−	9	6	4	67	67
Trial 2					
+/+	9	9	0	100	0
−/−	8	7	3	88	43
Combined					
+/+	15	12	0	80	0
−/−	17	13	7	76	54

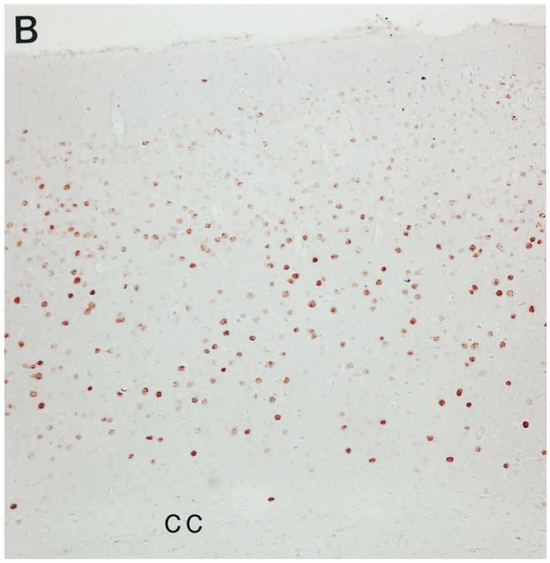
B
CC

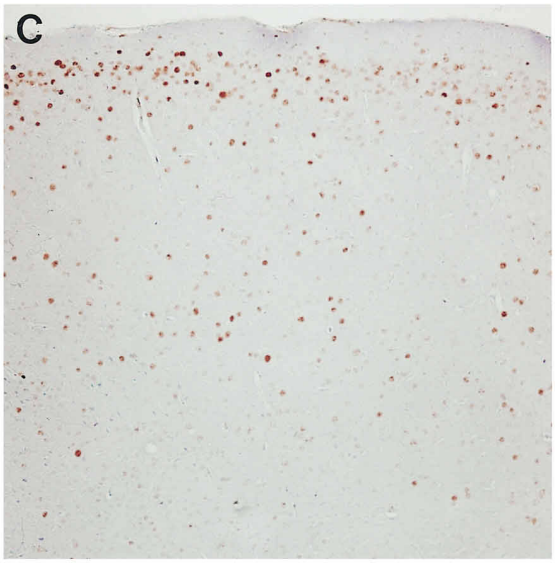
C

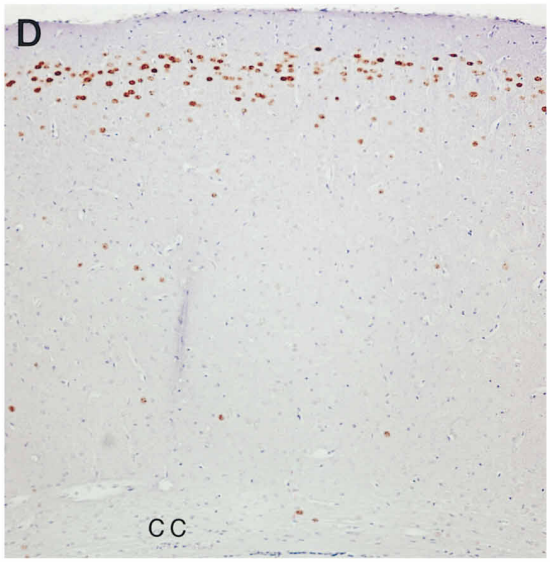
D
CC

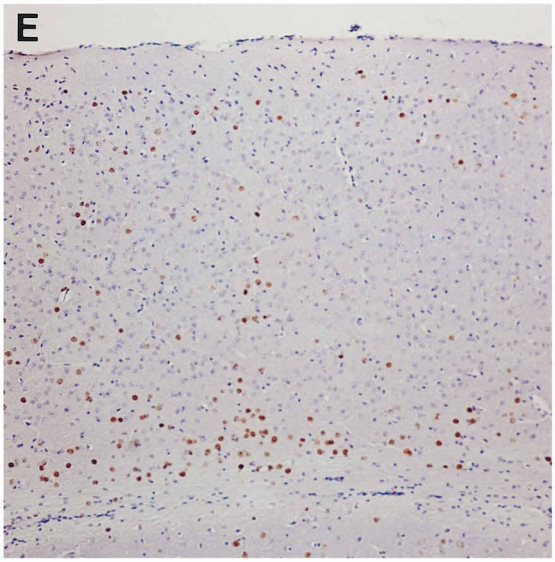
E

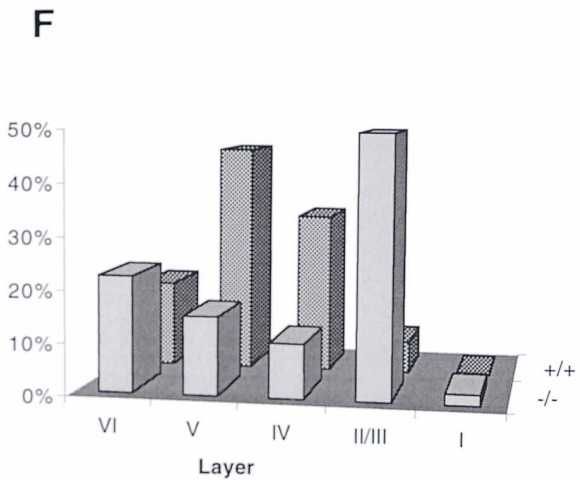
F
50%
40%
30%
20%
10%
0%
VI
V
IV
II/III
I
Layer
+/+
-/-

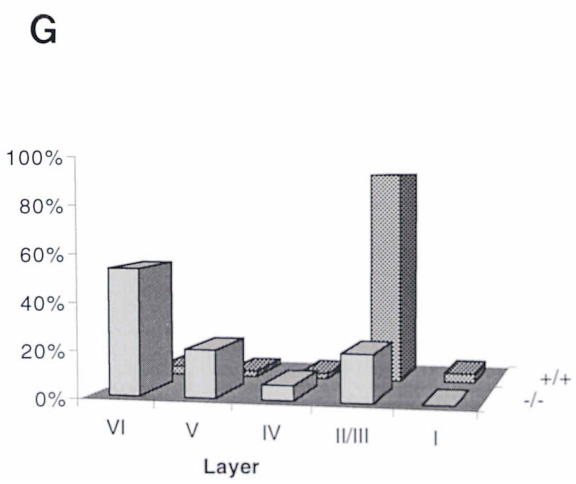
G
100%
80%
60%
40%
20%
0%
VI
V
IV
II/III
I
Layer
+/+
-/-

and extension of the hind limbs. Wild-type and mutant mice developed generalized convulsions with a similar frequency (80% and 76%, respectively), with an average latency time of 256 s for wild-type mice and 215 s for p35 mutant mice. Significantly, however, generalized convulsions led to no fatalities in wild-type mice, while >50% of p35 mutant mice died within minutes following cessation of the tonic-clonic phase of the seizure (Table 1). Wild-type and mutant animals that experienced generalized convulsions but did not die survived throughout the period of examination (5 days). The observations of p35 mutant mice seizing and the results of the PTZ seizure–induction experiments indicate that the mortality observed in the $p35^{-/-}$ population is likely to be due to seizures and not to a defect in somatic organs, which are histologically normal.

Discussion

We report the detailed analysis of the abnormalities in mouse strains harboring a homozygous deletion of p35, a neuronal-specific activator of cdk5. These mice display defects in patterning of all laminated structures of the CNS, in particular the neocortex. In addition, the aberrant axonal and dendritic trajectories are evident in p35 mutant mice. We demonstrate that the disrupted cortical lamination is the result of defective migration of postmitotic neurons. We also show that the unexpected mortality of p35 mutant mice can be explained by lethality due to seizures.

Mechanism of Cortical Defects

p35 is expressed in the entire CNS during embryonic development (Tsai et al., 1994; Tomizawa et al., 1996; Delalle et al., 1997). Its expression diminishes with the completion of neurogenesis in most structures of the CNS with the exception of the forebrain, where the expression of p35 persists into adult life. In the developing cerebral wall, high levels of p35 mRNA are evident in migratory neurons within the intermediate zone (Delalle et al., 1997) suggesting a role of the p35/cdk5 kinase in neuronal migration.

A salient feature of the structure of the adult mammalian cortex is the six distinct laminae that are formed by the successive migration of neurons past earlier-born neurons. Thus, neurons that occupy deep cortical layers are born early in corticogenesis while those that occupy superficial layers are generated later. The p35 mutant cortex exhibits an altered lamination pattern with typically deep-layer neurons present in superficial layers. Two possibilities might account for this observed abnormality. One possibility is that cell fate is altered in p35 mutant cortical neurons such that the birth-dating sequence is reversed, while the migration pattern of postmitotic neurons remains normal. A second possibility is that the migration pattern of cortical neurons is altered in the p35 mutant cortex, resulting in an inverted organization of cortical neurons (see Figure 6A). To distinguish between these possibilities, we performed a birth-dating experiment by injecting BrdU into timed pregnant females and determining the destination of labeled neurons in the adult offspring. In p35 mutant mice, we found that early-born neurons are present predominantly in superficial layers while neurons produced toward the end of corticocytogenesis localize mostly to deep layers (Figures 6C and 6E). These results cannot be easily explained by an alteration in cell fate of p35 mutant neurons. Rather, the mutant cortical neurons most likely follow a different migration pattern.

How is the nearly inverted cortical laminar structure caused by the altered migration of cortical neurons in the p35 mutant mouse? Examination of cortical structure during embryonic development reveals that in the E13 cerebral wall, the number and distribution of cells in the ventricular zone and the developing cortical plate are similar between the mutant and wild type (Figures 5A and 5B). However, 48 hr later, a discrepancy in cell distribution of the cerebral wall becomes obvious as the mutant cortical plate is 30%–50% thinner than the wild type and >50% more cells are present in the intermediate zone of the mutant cerebral wall (Figures 5C and 5D). Clearly, p35 mutant neurons at this stage already display defects in migration. The fact that cortical neurons move out of the ventricular zone at E13, that BrdU-labeled neurons are found in the intermediate zone at E15, and that individual neurons migrating along radial glial fibers could be visualized in the E17 cerebral wall using a modified Stensaas staining technique (1968; data not shown) suggest that the defect in migration is not related to impaired mobility of the cells. The migration defect is also unlikely to be related to the absence or abnormal distribution of radial glial fibers as the appearance and density of RC2-immunoreactive fibers are comparable between the wild type and p35 mutant (Figures 5E and 5F). Finally, the Cajal-Retzius cells in the marginal zone have been implicated in regulating migration of cortical neurons (Ogawa et al., 1995). MAP2 immunohistochemistry was performed on E13 cerebral walls to examine the configuration of neurons in the preplate, which subsequently splits into marginal zone and subplate. In wild-type and p35 mutant embryos, MAP2-stained cells are confined to the most superficial portion of the cerebral walls (data not shown). Thus, the Cajal-Retzius cells are most likely to be present in p35 mutant mice. Although it remains to be determined at which point during cortical development the p35/cdk5 kinase regulates neuronal migration, the densely packed neurons in the E15 $p35^{-/-}$ intermediate zone can be best explained by the inability of these neurons to migrate past the preexisting neurons in the cortical plate. As a consequence, throughout corticogenesis, neurons are packed from "outside-in" rather than the normal "inside-out" pattern. The inverse distribution of BrdU-labeled cells between wild-type and mutant mice in the E13 and E16 birth-dating experiments is consistent with this model.

Other Defects of the p35 Mutant Cortex

In addition to the disrupted laminar structure, the p35 mutant brain also features a diminished corpus callosum as well as the presence of aberrant fiber fascicles in the cortex. The aberrant fiber fascicles are likely to be composed of corticocortical, thalamocortical, corticobulbar, and corticospinal tracts. It is conceivable that

as the organization of cortical neurons is disrupted in p35 mutant mice, altered trajectories of efferents and afferents are created. We also cannot rule out the possibility that the altered trajectories and the reduced corpus callosum are the direct consequence of lack of p35. Golgi impregnation reveals that the radially aligned apical dendrites in the wild-type cortex are not observed in the p35 mutant cortex (Figures 3A and 3B). Furthermore, the normally upright position of pyramidal neurons displays an altered orientation, which subsequently results in a different plane of dendritic growth (Figures 3C and 3D). The abnormal orientation of dendritic growth could be influenced by the aberrant configuration of axonal fibers in the p35 mutant cortex.

Comparison of p35 Mutant Mice with *reeler* Mice

The autosomal recessive mouse mutant strain *reeler*, which displays neurological disorders and gait abnormalities, has been well characterized (Falconer, 1951; Goffinet, 1984; Caviness and Rakic, 1978; Rakic and Caviness, 1995). These mice exhibit defects in cortical lamination featuring an "outside-in" migration pattern during cortical development (Caviness, 1982; Caviness and Sidman, 1973; Hoffarth et al., 1995). Strikingly, Golgi analysis of *reeler* mice reveals an altered orientation instead of the normally upright position of pyramidal cells (Pinto Lord and Caviness, 1979). In addition, analysis of fiber patterns in the *reeler* neocortex indicates aberrant axonal trajectories sweeping through the cortex toward the pial surface of the brain (Caviness, 1976). These abnormalities highlight similarities between *reeler* and *p35*$^{-/-}$ cortical phenotypes. In fact, the "outside-in" migration pattern of *reeler* cortical neurons led to the hypothesis that later-born postmitotic neurons are unable to migrate past earlier-born neurons in order to occupy superficial positions (Caviness, 1982; Goffinet, 1984). Thus, p35 mutant mice and *reeler* mice may share what appears to be an analogous migration defect. However, differences are also apparent between the cortices of p35 mutant mice and *reeler* mice. For instance, the marginal zone (layer I) is missing in the *reeler* mice and present in p35 mutant mice. Furthermore, the corpus callosum is largely intact in *reeler* but diminished in the p35 mutant mice. The reeler mice also display cerebellum malformation and lamination defects in the hippocampal formation. Thus, p35 mutant mice display a phenotype that is similar to though milder than *reeler* in all noncortical structures (Figure 4). The full-length cDNA of the *reeler* gene product, reelin, was isolated and encodes a cell-surface or secreted protein sharing homology to extracellular matrix proteins involved in cell adhesion (D'Arcangelo et al., 1995; Ogawa et al., 1995).

Recently, a mouse strain harboring a homozygous deletion of the *cdk5* gene was created and displays late embryonic or perinatal lethality (Oshima et al., 1996). *cdk5*$^{-/-}$ mice exhibit an abnormal stratification of cortical neurons as well as those in the hippocampus. In addition, *cdk5*$^{-/-}$ mice lack foliation and layering in the cerebellum. While the defect in cortical lamination in *cdk5*$^{-/-}$ mice has yet to be characterized in detail, these results suggest that cdk5 may play a role in cortical lamination. In light of our observations that p35 mutant and *reeler* mice have analogous defects in cortical migration, we suggest that the phenotype displayed by cdk5 mutant embryos in the abnormal configuration in the cortex, hippocampal formation, and cerebellum is similar to that of *reeler* embryos. As a *p35* deletion causes a severe defect in the cortex, the other abnormalities presented in cdk5 mutant animals are likely to reflect the existence of other regulatory partners of cdk5, which compensate for the lack of p35 in p35 mutant animals. Indeed, a p35 homologue called p39 was recently isolated from a human hippocampus library (Tang et al., 1995). The similarities between the phenotypes of p35 and cdk5 mutant animals to those of *reeler* mice, in conjunction with the finding that *reeler* and p35 mutant mice share an analogous cortical migration defect, suggest that reelin, p35, and cdk5 might be in a common signaling pathway that regulates neuronal migration and laminar configuration. Alternatively, multiple mechanisms may exist to regulate neuronal migration during cortical development.

Adult Lethality and Seizures in p35 Mutant Mice

One reasonable consequence of the disrupted cytoarchitectonic structure of the cortex is that the altered pattern of cortical connections may lead to an increased susceptibility for having seizures. Indeed, p35 mutant mice suffer from seizure activity. In one instance, we observed the terminal portion of a generalized convulsion in a p35 mutant mouse, which died 2 days later. This particular observation raised the possibility that the 15% death rate in the p35 mutant population might be due to fatal seizures. To test this experimentally, seizures were induced in wild-type and p35 mutant mice using the convulsant PTZ. At 50 mg/kg body weight, PTZ induced generalized convulsions in wild-type and p35 mutant mice approximately 80% of the time. And though there was a slight decrease in the latency to onset of generalized convulsions in p35 mutant mice, the length of the convulsive episode was the same for both genotypes. Significantly, however, no deaths were associated with PTZ-induced seizures in wild-type mice, while in p35 mutant mice, PTZ-induced seizures were fatal >50% of the time. Thus, when seizures are induced experimentally with PTZ, p35 mutant mice are vastly more susceptible to dying from seizures than wild-type mice. The diminished ability of p35 mutant mice to recover from seizures is intriguing and awaits further investigation. The increased lethality of induced seizures, combined with observation of naturally occurring seizures in p35 mutant mice, strongly suggest that fatality due to seizures can explain the adult mortality in the *p35*$^{-/-}$ mouse population.

In the p35 mutant mouse, this finding of seizure activity causally related to a defect in cortical neuronal migration contains parallels to human neuronal migration disorders, of which the best known is lissencephaly of the Miller-Dieker type (Dobyns et al., 1992) that features malformation of the cortex and epilepsy. Thus, p35 mutant mice, which are viable, fertile, and display unique cytoarchitectonic defects in the cortex, not only serve as an ideal model system for studying the molecular

mechanism underlying cortical lamination but might also be valuable for studies of epilepsy.

Experimental Procedures

Production of p35 Mutant Mice

Screening of a 129/Sv mouse genomic library (Stratagene) with a PCR product encompassing the N-terminal 400 bp of the human *p35* open reading frame yielded one clone. Approximately 20 kb of genomic DNA insert was contained within the lambda phage vector Lambda Fix II. The entire insert was excised by digestion with NotI. The resultant 15 kb and 5 kb fragments were cloned into pBluescript SK (Stratagene). By Southern blot and sequencing, the 5 kb fragment was shown to contain the entire p35 open reading frame and 4 kb of downstream sequence. Furthermore, sequencing revealed that the open reading frame was continuous. To construct a targeting vector, 3 kb of downstream sequence and 5 kb of upstream sequence were cloned into the pPNT vector (Tybulewicz et al., 1991) to flank the neomycin resistance cassette. Thus, the entire *p35* ORF and 400 bp of downstream sequence were essentially replaced with the neo cassette in the opposite transcriptional orientation. A unique NotI site allows linearization of the targeting vector with the HSV-*tk* gene at one end of the linearized plasmid.

J1 ES cells (Li et al., 1992) were transfected with 30 μg of linearized targeting vector by electroporation (Bio-Rad Gene Pulser set at 400 V and 25 μF). Cells were grown in G418- (400 μg/ml) and FIAU- (0.2 μM) containing medium 24 hr after transfection. G418 resistance selects for homologous recombination events, which replace the *p35* coding region with the neo cassette. FIAU resistance selects against incorporation of the HSV-*tk* gene through random integration of the targeting construct into the genome. Following 9 days of selection, 196 resistant colonies were isolated and screened for homologous recombination events by Southern blot analysis. Genomic DNA from the clones were digested with BamHI and probed with a BamHI-XbaI 400 bp fragment (referred to as Probe A in Figure 1), which is external to the region of homology between the targeting vector and the *p35* locus. The wild-type allele yields a 6.5 kb fragment while the mutant allele yields a 6.9 kb fragment. Six positive clones were further confirmed by digestion with KpnI and Probe B (PstI-KpnI 500 bp fragment), which is internal to the region of homology between the targeting vector and the *p35* locus. The wild-type allele produces a 4.5 kb fragment while the mutant allele produces a 4.9 kb fragment. Two ES clones, 6D3 and 4C4, were chosen for injection into C57BL/6 host blastocysts for generation of chimeric animals.

Germ-line transmission of the mutation was determined by mating male chimeric animals to C57BL/6 females and confirmed by Southern blot analysis of tail genomic DNA of agouti offspring. Mice heterozygous for the mutation were interbred to generate homozygous mice. One 4C4 chimera displayed partial germ-line transmission and two 6D3 chimeras displayed full germ-line transmission of the mutation. One 6D3 chimera was bred to 129/Sv females to place the mutation in the 129/Sv inbred background. All mice were genotyped by Southern blot as described using either Probe A or B.

Western Blot and Kinase Assay

Whole brains of 4-week-old mice were dounce homogenized in lysis buffer containing 50 mM Tris-HCl (pH 7.5), 250 mM NaCl, 5 mM EDTA (pH 8.0), 0.1% Nonidet P-40, 5 mM DTT, 10 mM NaF, 1 mM PMSF, 1 μg/ml aprotinin, and 1 μg/ml leupeptin. Western blot analysis was performed on 25 μg and 50 μg of each lysate using an affinity-purified rabbit polyclonal antibody to p35. To assay for p35-associated kinase activity, 1 mg of protein from each lysate was immunoprecipitated with a monoclonal antibody to p35 and histone H1 was used as the substrate in in vitro kinase assays performed as previously described (Tsai et al., 1993). Each lysate (500 μg) was also immunoprecipitated with a rabbit polyclonal antibody to cdk5 (Santa Cruz), and kinase assays were again performed using histone H1 as the substrate.

Histology

Three-month-old mice were perfused with Bouin's fixative, and tissues were postfixed in Bouin's for at least 24 hr. All histological examinations were performed on age-matched littermates. Tissues were embedded in paraffin, sectioned at 4 μm, and stained with cresyl violet and luxol fast blue except where otherwise noted.

Reduced Silver Fiber Staining

Following perfusion and a week of fixation, adult mouse brains were frozen and sectioned coronally. The Fink-Schneider procedure (Fink and Heimer, 1967; Schneider, 1969) was essentially followed for reduced silver fiber staining and is described briefly here. Sections were rinsed in deionized water three times for 5 min each. They were then soaked in a solution of eight parts 2.5% silver nitrate and one part concentrated pyridine overnight to 48 hr. After sections were rinsed twice in 2.5% silver nitrate for 5 min each and once in deionized water for 3 s, samples were soaked for 3 min in a solution of 10 parts 2.5% silver nitrate to 1 part 9:6 mix of 2.5% sodium hydroxide to ammonia and then transferred to a Nauta-Gygax reducing solution (800 ml distilled water, 75 ml 95% alcohol, 17 ml 10% formalin, and 20 ml 1% citric acid) for 2 min. After rinsing, sections were transferred for 1 min to 0.5% sodium thiosulfate, rinsed again, mounted, dehydrated, and cover slipped.

Golgi Impregnation

For adult brain samples, the Golgi-Cox method as described by Brancroft and Stevens (1977) was followed. In brief, 3-month-old mice brains were dissected out, and the fresh tissue was placed in a solution of 10 ml 5% potassium dichromate, 10 ml 5% mercuric chloride, 8 ml 5% potassium chromate, and 40 ml water for 25–30 days. The tissues were then transferred to 5% sodium carbonate, dehydrated, embedded in low viscosity nitrocellulose, and cut at 100 μm on a sliding microtome.

Embryonic BrdU Analysis

All mice were maintained on a 12 hr light-dark schedule. Conception was ascertained by the presence of vaginal plug, with the day of conception considered to be embryonic day 0 (E0). Timed pregnant heterozygous mothers plugged by heterozygous male mice were sacrificed at gestational day E13 and E15, 30 min after intraperitoneal injection with BrdU at 50 mg/kg body weight. The brain of each embryo was dissected from the head and fixed overnight by immersion in 70% ethanol. After identification of genotype by PCR, embryonic brains were dehydrated in graded ethanol solutions, embedded in paraffin, and sectioned in the coronal plane at 4 μm. BrdU immunohistochemistry was performed according to standard procedures; anti-BrdU monoclonal antibody (Becton Dickinson) was used at 1:75 dilution at room temperature for 2 hr. Staining was developed using the Vectastain ABC kit. Sections were counterstained with basic Fuchsin as previously described (Takahashi et al., 1992).

Birth-Dating Experiments

For the E13 birth-dating experiment, an E13 pregnant heterozygous mother plugged by a heterozygous male mouse was given a single injection of BrdU intraperitoneally at 50 mg/kg body weight. For the E16 birth-dating experiment, an E16 pregnant heterozygous mother was given a series of five injections of BrdU intraperitoneally at 50 mg/kg body weight spaced 3 hr apart. Animals continued pregnancy and gave birth normally. At 1 month of age, wild-type and mutant animals born in each experiment were deeply anesthetized with a mixture of ketamine (50 mg/kg body weight) and xylazine (10 mg/kg body weight) and intracardially perfused with 4% paraformaldehyde, and the brains were removed. Brains were paraffin embedded and sectioned at 10 μm in the coronal plane. BrdU immunohistochemistry was performed essentially as described above and counterstained with cresyl violet.

RC2 Immunohistochemistry

RC2 immunohistochemistry was performed essentially as described in Misson et al. (1988). Cryostat sections (20 μm) were cut in the coronal plane of E17 wild-type and p35 mutant cortices and mounted on poly D-lysine coated slides. RC2 supernatant diluted 1:5 in phosphate-buffered saline containing 0.2% Triton X-100 was added to the sections overnight at 4°C. The next day, the slides were washed 3 × 10 min in a solution of 1% normal goat serum in phosphate-buffered saline. Anti-mouse IgM conjugated to biotin (Vector Laboratories) was added to the sections for 2 hr at room temperature. Staining was developed using the Vectastain ABC kit.

Quantitative Measurements

For the measurement of cortical cell density in Figures 2C and 2D, two photomicrographs of independent sections of each genotype

were divided into presumptive cortical layers. In each layer, the cell bodies present within a 100 μm^2 area were counted. Six "boxes" of 100 μm^2 were counted in each cortical layer (except layer I). The overall cell density represents the average number of cell bodies in each of 24 boxes counted from layers II/III to layer VI. To determine the number of BrdU-positive cells at E13 and E15, BrdU+ cells were counted in photomicrographs of coronal sections (three per genotype at E13, three per genotype at E15). The number of BrdU+ cells was divided by the area encompassing the ventricular zone and extrapolated to give the base units in cells/100 μm^2 area. The thickness of the cortical plate was measured in several different parts of the cortical plate in comparable sections of wild-type and p35 mutant E15 embryos. To determine the density of cells in the intermediate zone at E15, the number of cell bodies in a 56 $\times$ 56 μm box was determined in three areas in the intermediate zone of three photomicrographs per genotype. The cell density is the average of the measurements per genotype, extrapolated to give the base units in cells/100 μm^2 area. For quantitative measurements of BrdU-positive cells in the birth-dating experiments, comparable photomicrographs of sections of each genotype at E13 and E16 were examined. In each photomicrograph, cortical layers were identified and marked in wild-type sections, and the areas corresponding to these layers were marked in p35 mutant sections. BrdU+ cells were counted in at least three independent sections for each genotype at E13 and at E16. The average deviations from the mean in each layer at E13 were: +/+: 2.3% (VI), 1.6% (V), 3.2% (IV), 1.4% (II/III), and 0.3% (I); E13: −/−: 4.8% (VI), 2.2% (V), 1.5% (IV), 5.5% (II/III), and 1.4% (I). At E16: +/+: 0.8% (VI), 0.3% (V), 0.7% (IV), 1.1% (II/III), and 0% (I); E16: −/−: 4.1% (VI), 6.8% (V), 1.6% (IV), 1.7% (II/III), and 0% (I).

PTZ Seizure Induction

Adult wild-type and mutant mice aged 9–14 weeks were injected intraperitoneally with PTZ (Sigma) at 30 mg/kg body weight or 50 mg/kg body weight. All described observations were made during 2 hr immediately following the injection.

Experiments were performed blind to genotype. All surviving mice were euthanized 5 days after PTZ injection.

Acknowledgments

We thank Verne Caviness, Jr., Ivana Delalle, Pradeep Bhide, Michael Rivkin, Rosalind Segal, and Chris Walsh for discussion; Sherrie Witt and Thomas Benjamin for excellent technical assistance; Francis Jensen for advice regarding seizure experiments; Ed Harlow and Nick Dyson for partial support of this work; Lili Yamasaki for advice and support; Margareta Nikolic for technical assistance and all members of the Tsai laboratory for discussion and critical reading of the manuscript. Support for this work was provided by National Institutes of Health (NIH) grant P30-HD18655 to P. D., GM52106 to E. L., and GM53049 to L.-H. T., who is a Rita Allen Foundation Scholar.

Received November 4, 1996; revised November 11, 1996.

References

Angevine, J.B., and Sidman, R.L. (1961). Autoradiographic study for cell migration during histogenesis of cerebral cortex in the mouse. Nature *192*, 766–768.

Bancroft, J.D., and Stevens, A. (1977). Theory and practice of histological techniques. J. D. Bancroft and A. Stevens, eds. (New York: Churchill Livingstone Press), pp. 355–356.

Ben-Ari, Y., Tremblay, E., Richie, D., Ghilini, G., and Naquet, R. (1981). Electrographic, clinical and pathologic alterations following systemic administration of kainic acid, bicuculline or pentylenetetrazol: metabolic mapping using and deoxyglucose method with special reference to the pathology of epilepsy. Neuroscience *6*, 1361–1391.

Capecchi, M.R. (1989). Altering the genome by homologous recombination. Science *244*, 1288–1293.

Caviness, V.S., Jr. (1976). Patterns of cell and fiber distribution in the neocortex of the reeler mutant mouse. J. Comp. Neurol. *170*, 435–448.

Caviness, V.S., Jr. (1982). Neocortical histogenesis in normal and reeler mice: a developmental study based upon [^{3}H]thymidine autoradiography. Dev. Brain Res. *4*, 293–302.

Caviness, V.S., Jr., and Sidman, R.L. (1973). Time of origin of corresponding cell classes in the cerebral cortex of normal and *reeler* mutant mice: an autoradiographic analysis. J. Comp. Neurol. *148*, 141–152.

Caviness, V.S., Jr., and Rakic, P. (1978). Mechanism of cortical development: a review from mutations in mice. Annu. Rev. Neurosci. *1*, 297–326.

D'Arcangelo, G., Miao, G.G., Chen, S.-C., Soares, H.D., Morgan, J.I., and Curran, T. (1995). A protein related to extracellular matrix proteins deleted in the mouse mutant *reeler*. Nature *374*, 719–723.

Dellale, I., Bhide, P.G., Caviness, V.S., Jr., and Tsai, L.-H. (1997). Temporal and spatial patterns of expression of p35, a regulatory subunit of cyclin-dependent kinase 5, in the nervous system of the mouse. J. Neurocytol. In Press.

Dobyns, W.B., Elias, E.R., Newlin, A.C., Pagon, R.A., and Ledbetter, D.H. (1992). Causal heterogeneity in isolated lissencephaly. Neurology *42*, 1375–1388.

Falconer, D. (1951). Two new mutants. "trembler" and "reeler", with neurological actions in the house mouse. J. Genet. *50*, 192–201.

Fink, R.P., and Heimer, L. (1967). Two methods for selective silver impregnation of degenerating axons and their synaptic endings in the central nervous system. Brain Res. *4*, 369–374.

Goffinet (1984). Events governing organization of postmigratory neurons: studies on brain development in normal and reeler mice. Brain Res. Rev. *7*, 261–296.

Hellmich, M.R., Pant, H.C., Wada, E., and Battey, J.F. (1992). Neuronal cdc2-like kinase: a cdc2-related protein kinase with predominantly neuronal expression. Proc. Natl. Acad. Sci. USA *89*, 10867–10871.

Hoffarth, R.M., Johnson, J.G., Krushel, L.A., and van der Kooy, D. (1995). The reeler causes increased adhesion within a subpopulation of early postmitotic cortical neurons. J. Neurosci. *15*, 4838–4850.

Lew, J., and Wang, J.H. (1995). Neuronal cdc2-like kinase. Trends Biochem. Sci. *20*, 33–37.

Lew, J., Beaudette, K., Litwin, C.M.E., and Wang, J.H. (1992). Purification and characterization of a novel proline-directed protein kinase from bovine brain. J. Biol. Chem. *267*, 13383–13390.

Lew, J., Huang, Q.Q., Winkfein, R.J., Qi, Z., Aebersold, R., Hunt, T., and Wang, J.H. (1994). Neuronal cdc2-like kinase is a complex of cyclin-dependent kinase 5 and a novel brain-specific regulatory subunit. Nature *371*, 423–425.

Li, E., Bestor, T.H., and Jaenisch, R. (1992). Targeted mutation of the DNA methyltransferase gene results in embryonic lethality. Cell *69*, 915–926.

Luskin, M.B., and Shatz, C.J. (1985). Neurogenesis of the cat's primary visual cortex. J. Comp. Neurol. *242*, 611–631.

Mansour, S.L., Thomas, K.R., and Capecchi, M.R. (1988). Disruption of the proto-oncogene INT-2 in mouse embryo-derived stem cells: a general strategy for targeting mutations to non-selectable genes. Nature *336*, 348–352.

Meyerson, M., Enders, G.H., Wu, C.-L., Su, L.-K., Gorka, C., Nelson, C., Harlow, E., and Tsai, L.-H. (1992). A family of human cdc2-related protein kinases. EMBO J. *11*, 2909–2917.

Misson, J.-P., Edwards, M.A., Yamamoto, M., and Caviness, V.S., Jr. (1988). Identification of radial glial cells within the developing murine central nervous system: studies based upon a new immunochemical marker. Dev. Brain Res. *44*, 95–108.

Morgan, J.I., and Curran, T. (1991). Stimulus-transcription coupling in the nervous system: involvement of the inducible proto-oncogenes *fos* and *jun*. Annu. Rev. Neurosci. *14*, 421–451.

Morgan, J.I., Cohen, D.R., Hempstead, J.L., and Curran, T. (1987). Mapping patterns of c-fos expression in the central nervous system after seizure. Nature *237*, 192–197.

Nikolic, M., Dudek, H., Kwon, Y.T., Ramos, Y.F.M., and Tsai, L.-H. (1996). The cdk5/p35 kinase is essential for neurite outgrowth during neuronal differentiation. Genes Dev. *7*, 816–825.

Ogawa, M., Miyata, T., Nakajima, K., Yagyu, K., Seike, M., Ikenaka, K., Yamamoto, H., and Mikoshiba, K. (1995). The *reeler* gene-associated antigen on Cajal-Retzius neurons is a crucial molecule for laminar organization of cortical neurons. Neuron *14*, 899–912.

Ohshima, T., Ward, J.M., Huh, C.-G., Longenecker, G., Veeranna, Pant, H.C., Brady, R.O., Martin, L.J., and Kulkarni, A.B. (1996). Targeted disruption of the cyclin-dependent kinase 5 gene results in abnormal corticogenesis, neuronal pathology and perinatal death. Proc. Natl. Acad. Sci. USA *93*, 11173–11178.

Pinto Lord, M.C., and Caviness, V.S., Jr. (1979). Determinants of cell shape and orientation: a comparative Golgi analysis of cell-axon interrelationships in the developing neocortex of normal and reeler mice. J. Comp. Neurol. *187*, 49–70.

Rakic, P., and Caviness, V.S., Jr. (1995). Cortical development: view from neurological mutants two decades later. Neuron *14*, 1101–1104.

Schneider, G.E. (1969). Two visual systems. Science *163*, 895–902.

Stensaas, L.J. (1968). The development of hippocampal and dorsolateral pallial regions of the cerebral hemisphere in fetal rabbits. J. Comp. Neurol. *132*, 93–108.

Takahashi, T., Nowakowski, R.S., and Caviness, V.S., Jr. (1992). BrdU as an S-phase marker for quantitative studies of cytokinetic behavior in the murine cerebral ventricular zone. J. Neurocytol. *21*, 185–197.

Tang, D., Yeung, J., Lee, K.-Y., Matsushita, M., Matsui, H., Tomizawa, K., Hatase, O., and Wang, J.H. (1995). An isoform of the neuronal cyclin-dependent kinase 5 (cdk5) activator. J. Biol. Chem. *270*, 26897–26903.

Tomizawa, K., Matsui, H., Matsushita, M., Lew, J., Tokuda, M., Itano, T., Konishi, R., Wang, J.H., and Hatase, O. (1996). Localization and developmental changes in the neuron-specific cyclin-dependent kinase 5 activator (p35(NCK5A)) in the rat brain. Neuroscience *74*, 519–529.

Tsai, L.-H., Delalle, I., Caviness, V.S., Jr., Chae, T., and Harlow, E. (1994). p35 is a neural-specific regulatory subunit of cyclin-dependent kinase 5. Nature *371*, 419–423.

Tsai, L.-H., Takahashi, T., Caviness, V.S. Jr., and Harlow, E. (1993). Activity and expression pattern of cyclin-dependent kinase 5 in the embryonic mouse nervous system. Development *119*, 1029–1040.

Tybulewicz, V.L.J., Crawford, C.E., Jackson, P.K., Bronson, R.T., and Mulligan, R.C. (1991). Neonatal lethality and lymphopenia in mice with a homozygous disruption of the c-abl proto-oncogene. Cell *65*, 1153–1163.